Photoinduced second-harmonic generation of $YBa_2Cu_3O_{7-delta}$ single crystals

1994 J. Phys.: Condens. Matter 6 4119

(http://iopscience.iop.org/0953-8984/6/22/011)

J. Phys.: Condens. Matter 6 (1994) 4119–4128. Printed in the UK

Photoinduced second-harmonic generation of $YBa_2Cu_3O_{7-\delta}$ single crystals

I V Kityk
Physics Department, Lviv University, Yaroslavenko 47/31, Lviv-34, 290034, Ukraine

Received 26 October 1993, in final form 7 January 1994

Abstract. Complex investigations of the photoinduced changes in $YBa_2Cu_3O_{7-\delta}$ ($\delta > 0.5$) single crystals have been carried out using the time-resolved dependences of the photocurrent, photoresistivity, photovoltage and optical second-harmonic generation (SHG). Simultaneously the spectroscopic parameters were monitored by time-resolved Raman and UV–visible reflection spectra. A time delay shift between the SHG and photocurrent dependences was found. The contributions of two different mechanisms in the formation of the superconducting behaviour were unambiguously shown. It was clearly shown that only by simultaneously taking into account the anharmonicity due to the specific electron–phonon interaction together with the traditional Anderson metal–insulator transition we can clarify the main physical mechanisms of the high-temperature superconductivity. Magnetic fields of up to 1 T suppress the SHG signal. The different delay times for the electronic and phonon spectra indicate the essential role of the electron–phonon anharmonic coupling in the high-temperature superconductivity. Some different approaches to explain the observed phenomena are discussed.

1. Introduction

The very interesting phenomenon that the photodoping of $YBa_2Cu_3O_{7-\delta}$ ($\delta > 0.5$) single crystals yields large photoinduced changes in resistivity was recently observed [1–7]. In particular, during laser photoexcitation, insulating samples of $YBa_2Cu_3O_{7-\delta}$ ($\delta > 0.5$) become highly conducting. Yu *et al* [8] have performed time-resolved experiments on single crystals of $YBa_2Cu_3O_{6.3}$ and found a linear dependence of the photocurrent (PC) peaks for light intensities up to 5×10^{15} photons cm^{-2}. However, for intensities above 6×10^{15} photons cm^{-2}, superlinear behaviour was found, which indicates that there is an additional transport mechanism. At the same time, a decrease in the transient resistance at 50 K by more than 14 orders of magnitude was observed. Moreover, the photoinduced conductivity was time delayed with respect to the absorption. The deep photoinduced resistivity minimum below 100 K, which is related to the onset of superconductivity in granular superconductors and in inhomogeneously doped samples, was interpreted in terms of phase separation and metallic droplet formation. It was also shown that the heating is not the dominant factor in such experiments because, to obtain the observed change in resistivity due to heating, the change in temperature should exceed the melting temperature.

Kityk *et al* [7] have performed complex investigations of the photoinduced changes in $YBa_2Cu_3O_{7-\delta}$ single crystals. Low-power He–Ne, He–Cd, He–Se and N_2 lasers and YAG:Nd and XeCl pulsed lasers were used as the laser power sources. Crystalline samples in both superconducting and semiconducting phases were chosen for the investigations. Quite strong dependences of the non-stoichiometry parameter $7 - \delta$ on the laser power, wavelength and external conditions were observed. The oxygen number $7 - \delta$ showed

0953-8984/94/224119+10$19.50

a tendency to increase for the initially semiconducting phase and to decrease for the superconductors. The most interesting results were obtained using the XeCl excimer laser, where the corresponding changes were observed only under an applied hydrostatic pressure (up to 20 MPa) in an oxygen atmosphere. In all cases the penetration depth of the new induced superconducting phase was 5.5–6.5 μm. It was shown also that, for high light intensities (above 5×10^{18} photons cm^{-2}), heating can play an important role and is superimposed on the breaking of the corresponding electronic bonds. In the latter case, investigation of the contribution of different mechanisms is very difficult and the origin of such phenomena is still not understood.

As well as the applied aspects, the photoinduced investigations play a great role in the deeper understanding of the origin of high-temperature superconductivity. In particular, Emery and co-workers [9, 10] and Grilli *et al* [11] have theoretically predicted that the hole mobility initiated by photodoping is inhibited by the phase-separated droplets. Their approach was based within two-dimensional antiferromagnetic ordering. Dilute holes are unstable against phase separation into a hole-rich phase and a pure antiferromagnetic insulating phase. Moreover, it was argued that dynamic phase separation (fluctuations in the carrier density at intermediate scales) can lead to BCS pairing. This causes a diffusion-limited carrier mobility and thereby the photoconductance.

Kityk [12] has investigated the temperature behaviour of second-harmonic generation (SHG) and demonstrated that SHG is a very sensitive method of high-T_c diagnostics. It was revealed that, when the temperature decreases towards the superconducting transition temperature T_c, the SHG signal increases smoothly, appearing almost completely at temperatures near T_c. At the same time, the volume origin of SHG was elucidated. SHG measurements were performed for different geometries and polarizations of the incident and reflected laser beams, which indicated the crystalline origin of the observed effect.

The absolute values of the tensor components $\chi_{123}^{(\omega,\omega)}$ were low and equal to a maximum of about 10^{-15} m V^{-1}, which suggests that this effect is forbidden by the macrosymmetry. Perhaps the corresponding phenomena are caused by the local disordering with a very long-range structural modulation, very similar to what takes place in incommensurate phases. The symmetry of such a weak long-range distortion can be acentric; so phenomena describable by third-rank polar tensors can be observed.

To check this idea, Kityk [12] measured the structural parameters and revealed that, in the temperature range 20–72 K, two structural phases coexist simultaneously. The first, the stronger, belongs to the space group D_{2h}^{17} and the second to the acentric C_{2v}^{6} phase. Weak x-ray scattering satellites $(k, l \pm \zeta, m)$ with $\zeta = 0.08$–0.10 were also observed. The origin of this behaviour is not quite clear, but the observed structural modulation can indicate the possibility of the existence of an incommensurate phase. In [12] the possibility of using SHG methods for the detection of the onset of superconductivity was shown unambiguously.

In interpreting the results obtained, it is very important to carry out the complex time-dependent study of the SHG, resistivity and PC simultaneously. Together with the time-dependent PC and SHG experiments in this report we shall present time-resolved spectroscopic data (in the visible–UV and Raman phonon spectral ranges), which are intrinsic to a deeper understanding of the origin of the high-temperature superconductivity. In the present author's opinion, only such wide investigations can clarify the main mechanisms of the photoinduced phenomena and probably give more detailed information about high-T_c features, particularly concerning the role of electron–phonon interactions. All the measurements were performed in the high-time resolution regime and over a wide temperature range. On the other hand, from the material scientist's point of view, photoinduced changes can be used to create finely dispersed defects which form pinning

centres of the magnetic flux in Y–Ba–Cu–O materials. There also appears the possibility to design high-time-resolved laser switches.

2. Experimental details

The flux technique was used to grow $YBa_2Cu_3O_x$ single crystals. $BaCO_3$ and CuO in the molar ratio 6:17 were used as the flux materials. A mixture of flux and Y–Ba–Cu–O in the weight ratio of 3.5:1 was melted at 1290 K and slowly cooled to 1095 K at a rate of 2–4 K h^{-1}, employing a vertical furnace coupled with a programmed controller. The size of the crystal surface was 2 mm × 2 mm. The parameter x was checked by x-ray diffraction. Superconducting behaviour was estimated also by measuring the resistance as a function of temperature. The samples were placed in a thermoregulated helium cryostat and illuminated using different laser sources. The PC was measured by the standard four-probe method.

Time-dependent optical spectra, including Raman, IR and visible reflection spectra, were measured simultaneously. The Raman spectra were obtained using Ar lasers as the source. The reflection coefficients were measured using Specord-M40 and SF-26 spectrophotometers, which were coupled with the high-time-resolved spectroanalyser SA-107 (Burgunds Ltd Co).

In this report an experimental investigation of the photoinduced changes caused by nitrogen laser (λ = 337 nm) UV irradiation with a pulse width of about 650 ps will be presented. The instrumental resolution (rise time) was about 150 ps. Samples were irradiated using focused pulsed nitrogen laser UV light with a photon flux less than 6×10^{18} photons cm^{-2}. This power restriction is caused by the necessity of avoiding sample heating, which occurred in the experiments described by Kityk *et al* [7]. The transmission and reflection spectra of the samples were recorded using a Specord-M40 spectrophotometer connected with a synchroamplifier.

As usual, the Auston-switch configuration was used to control the transient PC. The samples under investigation were placed on a 75 Ω stripline transmission line formed by evaporated Ag. The voltage of the DC bias sources was varied from 0 to 7 V and the corresponding line was connected to a boxcar detector. The corresponding device allows a high-frequency response to be obtained up to 180 GHz. The gate width of the boxcar was chosen as 35 ps for the PC at times less than 15 ns, and for time evolution measurements in the range from 20 ns to 1000 μs the gate width was selected to be from 8 to 25 ns.

The intensity of the nitrogen laser was varied using neutral density filters. The laser intensity at the sample position was controlled using a commercial fast-response joulemeter (Genetic, Inc., model ED-200). To avoid the bolometric effect or thermal effect a relatively weak laser intensity of 5–9 mJ cm^{-2} was used. A quantitative estimation based on standard heat transfer calculations shows that the photogenerated temperature rises by a few kelvins and is dissipated within 80–120 ns. The known heat data of $YBa_2Cu_3O_{7-\delta}$ measured by Lagreid *et al* [13] and Hagen *et al* [14] were used. From our calculations we conclude that, under the present experimental conditions, thermal equilibrium is established within 80–120 ns.

To measure the PC and resistivity, indium contacts were soldered onto two opposite faces of the sample to determine the photoconductivity in the two-probe geometry.

An apparatus for SHG was set up with an unfocused beam from a single-mode picosecond YAG:Nd laser (W = 30 MW; λ = 1.06 μm). The angle of incidence was varied from 2° to 48° to the surface normal. The plane of polarization of the pump light was rotated by a pair of Fresnel rhombs (Nicol prism). The separation between the SHG and the pump light

was achieved using an SMR-12 grating monochromator. The SHG intensity was measured using an FEU-79 photomultiplier. The measurements were carried out in the single-pulse regime, with a pulse frequency repetition of 12 Hz. As an intensity standard we used a quartz single-crystal cell in the plane of the optic axis. The crystal was mounted in a temperature-regulated cryostat for smooth variations of temperature in the range 4.2–300 K.

3. Results and discussion

For the investigations we used insulating $YBa_2Cu_3O_{6.45}$ single crystals with a resistivity of about 2×10^2 Ω cm at room temperature, increasing at lower temperatures to 9×10^8 Ω cm. It was revealed that the SHG response is independent of the pulse width. This indicates the absence of thermal influence on the corresponding photoinduced changes, because the heating will tend to make the time-dependent SHG signal width vary.

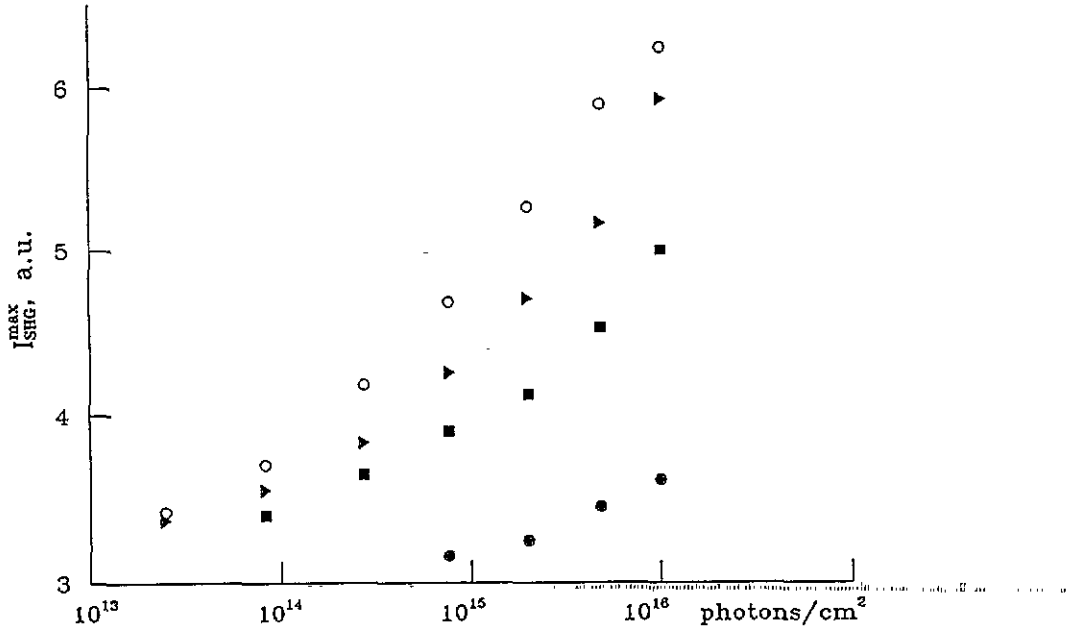

Figure 1. Dependences of the SHG intensities (a.u., arbitrary units) of $YBa_2Cu_3O_{7-\delta}$ from the *nitrogen laser photon flux for different oxygen deficiencies (liquid-nitrogen temperature):* ●, $\delta = 0.79$; ■, $\delta = 0.75$; ▲, $\delta = 0.64$; ○, $\delta = 0.55$.

It is well known that the SHG phenomena can occur only in acentric media, but $YBa_2Cu_3O_{7-\delta}$ single crystals in both phases (normal and superconducting) are centrosymmetric. Therefore the photoinduced non-linear optical phenomena are forbidden by symmetry. However, the appearance of acentric crystalline components occur owing to the existence of the specific electron–phonon interaction.

The non-linear optical response of the surface layer of a centrosymmetric crystal at the frequency of SHG is usually described as the sum of the quadrupole polarization $P^Q(2\omega)$ and the dipole polarization $P^D(2\omega)$. The first term is caused by the spatial dispersion and

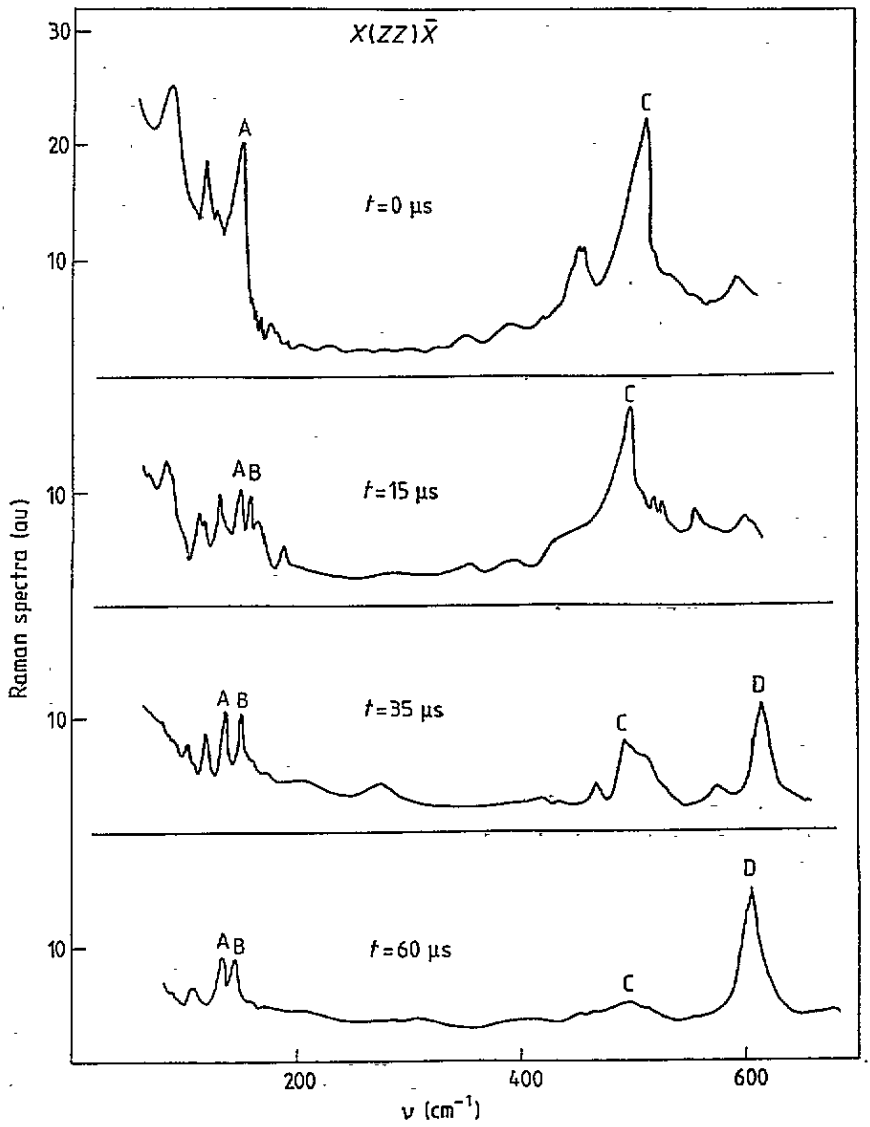

Figure 2. Raman spectra (a.u., arbitrary units) at different times after laser illumination for the $X(ZZ)\bar{X}$ scattering geometry.

by the discontinuity in the normal component of the field $E(\omega)$ at the interface. The second term arises from the surface layer of the semiconductor with broken inversion symmetry with a thickness of a few lattice constants.

From figure 1, one can clearly see that, as the temperature increases, the corresponding SHG intensity is very sensitive to the laser power. Moreover, this dependence has sublinear features. Such a non-linearity reflects the intrinsic role of the electronic subsystem which is perturbed by the non-linear electron–phonon interaction. At the same time, the corresponding SHG signal tends to increase with increase in the oxygen concentration.

To investigate the influence of the phonon subsystem, time-dependent Raman

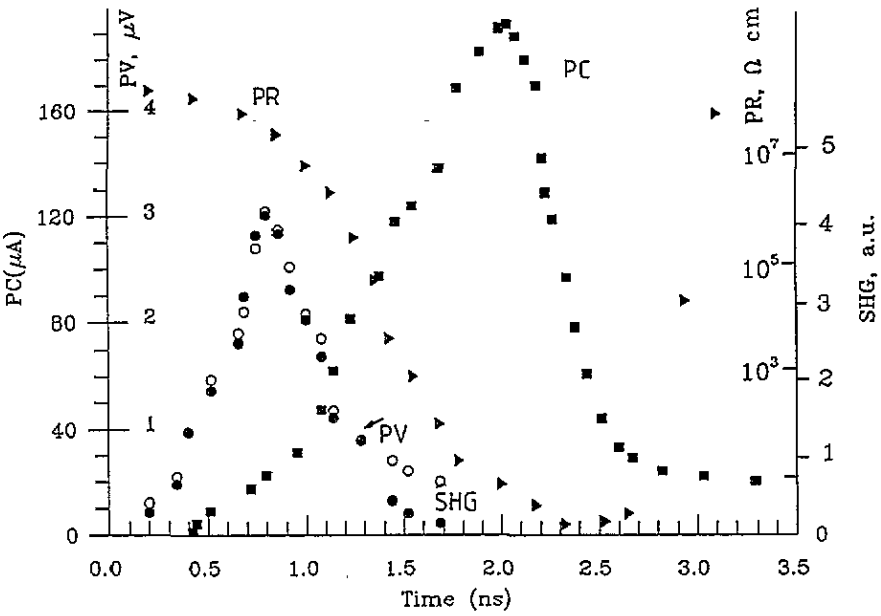

Figure 3. Time dependences of the SHG intensity (a.u., arbitrary units), photovoltage (PV), PC and photoresistance (PR) for the $YBa_2Cu_3O_{6.45}$ samples at liquid-nitrogen temperature.

measurements were carried out. From figure 2 it is clearly seen that mode D increases in frequency as the time after illumination increases. However, the structure of the spectra near modes A and B, which are assigned to cation vibrations, is very complex. The results obtained are in good agreement with the Raman spectra obtained by Burns *et al* [15], who measured the Raman spectra of $YBa_2Cu_3O_{7-\delta}$ as a function of oxygen concentration. It was revealed that for $\delta = 1$ the usual five *c*-axis polarized modes were observed. The mode near 500 cm^{-1} is primarily due to motion of oxygen atoms in the four-coordinated Cu chain. At oxygen contents near the metal–insulator phase transition, the intensity of this mode decreases and then vanishes, being replaced by a strongly polarized mode in the vicinity of about 600 cm^{-1}. The mode at 600 cm^{-1} probably corresponds to vibrations of two-coordinated Cu 'sticks'. Therefore the experimental data presented in figure 2 show unambiguously that the relaxational time of the phonon subsystem is more than three orders longer than that of the electronic subsystem. Therefore, for more complete understanding of time-dependent superconducting properties, it is necessary to take into account the influence of the electron–phonon interaction.

The SHG peaks as well as the transient PC were measured with the samples at different temperatures. It was found that in the temperature region 4.2–100 K the shift between the SHG and PC maxima remains almost unchanged, but with increasing temperature up to 100 K the SHG peak smoothly vanishes. The time-resolved SHG and PC behaviours of $YBa_2Cu_3O_{6.45}$ single crystals at liquid-nitrogen temperature together with the corresponding dependences of the resistivity and photovoltages are shown in figure 3. One can clearly see the delay in the SHG intensity with respect to the pump nitrogen laser light up to 1.3–2.0 ns. All results were obtained after averaging the measured data over 8000–12 000 pulses. The time asymmetry of the SHG curve is very interesting. The weak photovoltaic signal serves as the internal detector of the pump pulse at the same instrumental resolution. By comparing the time evolution of the SHG and the corresponding PC, one can clearly see the delay in

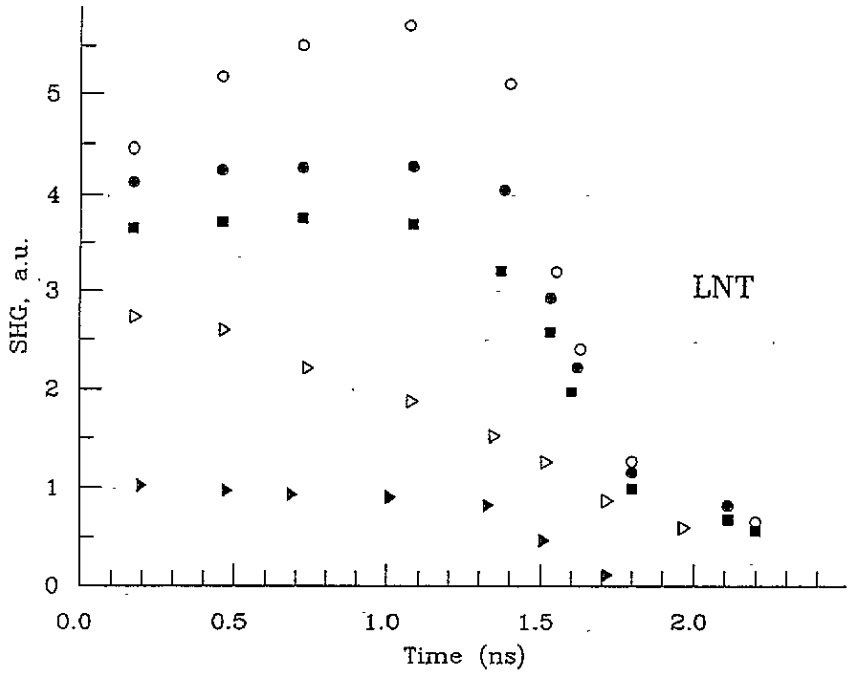

Figure 4. Time dependences of the SHG intensities (a.u., arbitrary units) for different nitrogen laser photon fluxes at liquid-nitrogen temperature: ▲, 10^{13} photons cm^{-2}; △, 4×10^{14} photons cm^{-2}; ■, 6×10^{15} photons cm^{-2}; ●, 3×10^{16} photons cm^{-2}; ○, 2×10^{17} photons cm^{-2}.

the SHG signal relative to the photovoltaic dependence, which indicates that the SHG tail is delayed by up to 1 ns.

The time variation in the SHG maximum at liquid-nitrogen temperature for different laser intensities is presented in figure 4. One can clearly see the occurrence of maxima in the time dependence of the SHG maximum. It was also found that the sample resistivity decreased from its starting value by more than seven orders, but for the deeper (more than 100 μm thickness) layer this value was reduced to only 2×10^2–10 Ω cm, which reflects the absorption of the light.

Dovgii *et al* [16] have introduced the spectroscopic parameters of high-T_c superconductors. They showed that the spectral peaks at 1.77 and 4.11 eV are more sensitive to the disappearance of the high-T_c parameters.

The time variation of one of the peaks (that at 4.08 eV) is shown in figure 5, which indicates the appearance of the dielectric phase. It is necessary once more to note that the Raman spectra changes more slowly with time (see figure 2) compared with the electron subsystem. These differences can be explained only by the different influences of the pump light on the phonon and electron subsystems.

To understand this behaviour, in the present author's opinion it is very important to note the intrinsic role of the apex oxygen in the phase transition to superconductivity [17–19]. It was revealed that the vibration of O(4) atoms normal to the CuO_2 plane is closely related to the strong fluctuations of charge along the c axis and electron (hole) transfer between these planes and chains of CuO.

Moreover Plakida and co-workers [20, 21] have shown that one of the main causes of the occurrence of superconductivity is the strong interaction between the electrons and the

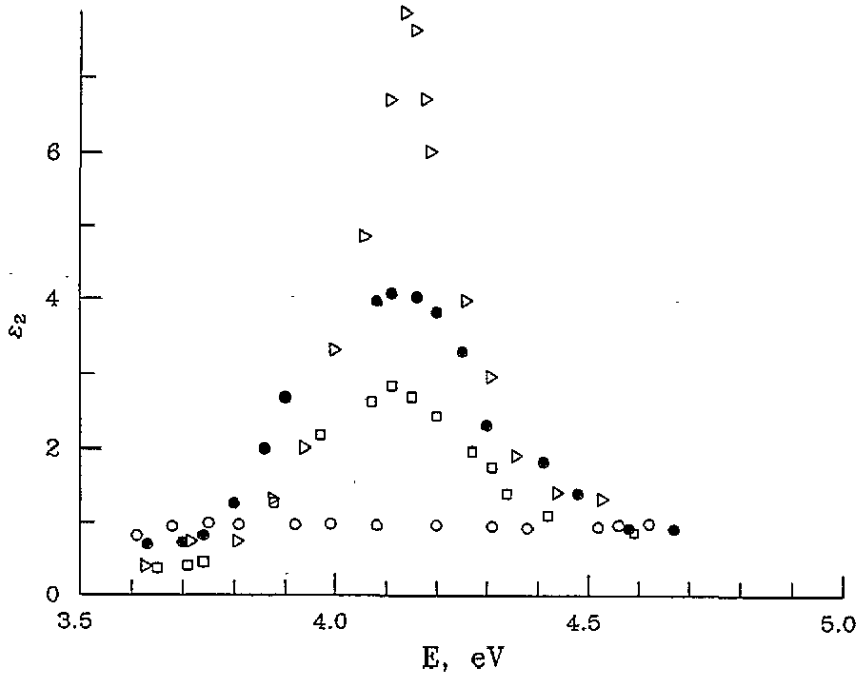

Figure 5. Spectral behaviour of the maximum of the imaginary part of the dielectric susceptibility ε_2 in the vicinity of the analytical spectral lines at different times after illumination: ○, 10 ns; □, 25 ns; ●, 50 ns; △, 85 ns.

local anharmonic vibrations. The interaction of electrons with the anharmonic vibration mode leads to the appearance of two subbands and causes their additional narrowing with the simultaneous frustration of the exchange interaction. The electron contribution to the non-linear optical susceptibilities described by the third-rank polar tensor, arising because of the electron charge transfer from the CuO layer, more probably plays an intrinsic role in the appearance of the non-linear optical response. The results obtained in this work suggest that the above theoretical approach can clarify the origin of the high-temperature superconductivity in future.

Because the third-rank non-linear optical susceptibilities are determined by the matrix dipole elements to explain the observed delay it is necessary to describe the time-dependent behaviour of the matrix elements due to the electron–phonon interaction.

It is necessary to note that Yu *et al* [8] explain the observed delay in the PC by the low mobility of free carriers due to their self-localization in disordered antiferromagnetic phase.

Photoexcitation (up to 5×10^{18} photons cm^{-2}) creates a large number of carriers which shifts the Fermi energy and causes screening, leading to a localization length related to the conductivity and optical spectra. On the other hand, the excitation at 3.7 eV tends to displace the oxygen atoms partly (clearly shown in figure 2) which is revealed in the metastable states with a long relaxation time (up to 10–20 μs).

Such an unusual behaviour of the electron and defective subsystem leads to time-dependent changes in the mixed (electron–phonon) wavefunctions, which determine the peculiarities of the SHG and corresponding optical parameters. The difference between the relaxation times for the atomic (defective) and electronic states is caused by the inhomogeneity of the system. In the latter case the atomic displacements (first of all the

apical oxygen atoms) partly due to the breaking of the chemical bonds lead to migrations of the corresponding atoms. In this case the site symmetry of the oxygen changes from twofold to fourfold coordination. The occurrence of the third-order rank tensor indicates the onset of acentricity in the electron charge density distribution, which can appear only because of the electron–phonon anharmonicity, as described above.

At the same time, phase separation between disconnected hole-rich regions separated by the insulating regions plays a very significant role in the processes mentioned. The absorbed photons create electron–hole pairs in the CuO_2 planes; the electrons will be quickly trapped at oxygen vacancies on adjacent partially oxidized CuO chains and tend to enhance the orthorhombic distortion locally, as observed in the photoinduced absorption experiments [8].

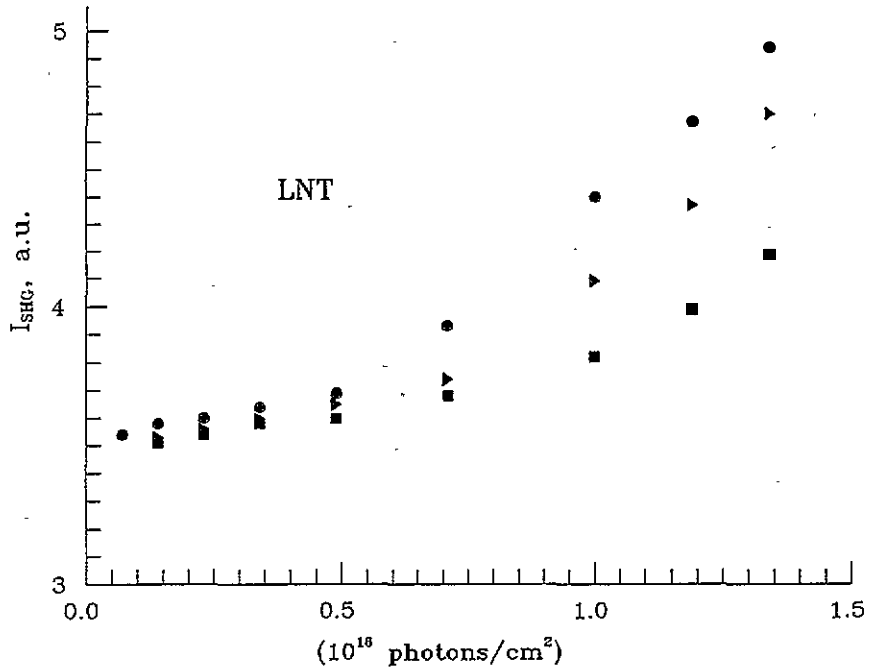

Figure 6. Dependences of the SHG intensities (a.u., arbitrary units) of $YBa_2Cu_3O_{7-\delta}$ from the nitrogen laser photon flux at different magnetic fields at liquid-nitrogen temperature: ●, 0 T; ▲, 0.45 T; ■, −0.79 T.

On the other hand, the hole mobility is restricted by the antiferromagnetic long-range spin ordering; so the observed insulator–metal transition can be explained by the intrinsic phase separation of the photogenerated carriers and metallic droplet formation in the antiferromagnetic insulators. The observed metastability is consistent with the phase separation in the metallic region. Analogous results [8] are obtained using theory of the Anderson order–disorder transition.

Lagreid *et al* [13] and Grilli *et al* [10, 11] have investigated theoretically the influence of the antiferromagnetic ordering and predicted the suppression of the corresponding superconducting phenomena. To check this prediction in the present work, all the above features were measured in a magnetic field. It was suggested that the magnetic field

suppresses the SHG maxima (figure 6), which once more indicates the close connection between the appearance of superconductivity and the onset of the SHG. However, the Raman and optical spectra obtained did not show any essential changes. Such behaviour reflects the intrinsic role of the antiferromagnetic ordering in the appearance of the acentric components together with the anharmonicity due to the specific electron–phonon interaction.

4. Conclusion

The results obtained have both theoretical and applied importance. Using laser photodoping, one can switch Y–Ba–Cu–O materials between the insulating and superconducting phases within a very short time period (of the order of nanoseconds). On the other hand the results obtained are important for a deeper understanding of the appearance of BCS pairing due to dynamic phase separation (and specific electron–phonon anharmonicity). It was clearly shown that only simultaneously taking into account the anharmonicity due to the specific electron–phonon interaction together with the traditional Anderson metal–insulator transition can clarify the main physical mechanisms of the occurrence of high-temperature superconductivity.

Acknowledgments

I would like to thank B Abramovitz and J Filkenshtein for help in carrying out the measurements. I am grateful to Professor F Sorge, Professor Y Uesu, Professor R V Lutciv, Professor E Shachinger and Professor I V Stasyuk for a valuable discussion of the results obtained.

This work was supported by the Ukrainian Committee of Science and Technology.

References

[1] Taliany C, Zamboni K, Ruani G and Matacotta F C 1989 *Synth. Met.* **29** F585
[2] Yu G, Heeger A J, Stucky G, Herron N and McCarron E M 1989 *Solid State Commun.* **72** 345
[3] Yu G, Heeger A J, Herron N and McCarran E M 1991 *Phys. Rev. Lett.* **67** 2581
[4] Thio T, Birgeneen L, Cassaho A and Kastner M A 1990 *Phys. Rev.* B **42** 10800
[5] Kudinov V I, Kreines N M, Kirilyuk A I, Laiho K and Lahdermta B 1990 *Phys. Lett.* **151A** 358
[6] Yu G, Lee C H, Heeger N and McCarron E M 1992 *Phys. Rev. Lett.* **67** 2581
[7] Kityk I V, Lutciv R V, Malynych S Z and Vasyuk N M 1993 *Acta Phys. Pol.* A **84** 609
[8] Yu G, Lee C H, Heeger A J, Herron N, McCarran E M, Lin Cong, Spalding G C, Nordman C A and Goldman A M 1992 *Phys. Rev.* B **45** 4964
[9] Emery V J, Kivelson S A and Lin H Q 1990 *Phys. Rev. Lett.* **64** 475
[10] Emery V J and Kivelson S A 1993 *Physica* C **209** 597
[11] Grilli M, Raimondi R, Castellani C, DiCastro C and Kotliar G 1991 *Phys. Rev. Lett.* **67** 253
[12] Kityk I V 1993 *Phys. Status Solidi* b **180** K35
[13] Lagreid T, Fossheim K, Sandvold E and Julsrud S 1987 *Nature* **330** 637
[14] Hagen S J, Wang Z Z and Cug N P 1989 *Phys. Rev.* B **40** 9389
[15] Burns G, Dacol F, Feild C and Hotzberg F 1991 *Physica* C **181** 37
[16] Dovgii Ya O, Karplyuk L T, Kityk I V, Nosan A V, Lutciv R V and Koterlyn M D 1990 *Dokl. Akad. Nauk. USSR* A **63** (in Russian)
[17] Kwei G H, Larson A C, Hults W L and Smith G L 1990 *Physica* C **160** 524
[18] Conradson S D and Raistrick I D 1990 *Science* **248** 1394
[19] Stasyuk I V and Shvaika A M 1993 *Acta Phys. Pol.* **84** 293
[20] Plakida N M, Aksenov V L and Drechsler S L 1989 *Europhys. Lett.* **4** 1309
[21] Plakida N M 1989 *Phys. Scr.* **29** 77